The conceptual design of SCal: A facility calibration system for the Maunakea Spectroscopic Explorer

Luke M. Schmidt[a], Jennifer L. Marshall[a], Darren L. DePoy[a], and Samuel C. Barden[b]

[a]Department of Physics and Astronomy Texas A&M University, 4242 TAMU, College Station, TX 77843-4242 USA

[b]The Maunakea Spectroscopic Explorer Project Office, 65-1238 Mamalahoa Hwy Kamuela, HI 96743 USA

ABSTRACT

The Maunakea Spectroscopic Explorer is designed to obtain > 4000 simultaneous spectra from the optical to NIR over a 1.5 square degree field of view at multiple resolutions and with unprecedented sensitivity (m=24). A robust facility science calibration system (SCal) will be required to achieve the desired precision over many observations spaced across months or years with minimal impact to the observing efficiency. We describe the major hardware components required to perform sensitivity and wavelength calibrations, removal of sky background and other stray light or ghost signals, PSF calibration, and detection of any spurious contamination sources.

Keywords: Massively multiplexed spectroscopic surveys, 10m-class telescopes, spectroscopic facility, survey facility, wide field, multi-object spectrograph, calibration

1. INTRODUCTION

The SCal conceptual design has drawn inspiration from several large-scale fiber positioner spectroscopic survey projects such as 4MOST,[1] PFS,[2] and DESI[3] that are at a later stage of development than MSE. To achieve the stated MSE goals (m=24 sensitivity limit, sky subtraction to better than 0.1%) over many targets in each field, and survey observations over the course of several years represent a significant challenge.

The MSE Science Calibration Unit (SCal) is comprised of light sources, fiber bundles, projectors, and optical systems required to focus, collimate, or otherwise modify the calibration light to maximize system efficiency. This system also includes means of detecting spurious contamination, such as LEO satellites crossing an individual fiber. Top level considerations for the designs described in this document are maximizing efficiency to minimize the calibration overhead and ensure the majority of observing time is spent collecting scientific spectra, not performing calibration. Likewise minimizing moving parts and utilizing commercially available hardware where possible helps improve reliability and reduces the overall cost of SCal.

This paper is a summary of the results of a conceptual design study for the Scientific Calibration (SCal) subsystem for the Maunakea Spectroscopic Explorer. This study was undertaken between November 15, 2020, and March 8, 2022. Work was focused on identifying only the light sources, optics, optomechanics, and other hardware required to perform the expected calibration tasks for the Maunakea Spectroscopic Explorer. The MSE science requirements flow down to the SCal system requirements has not yet been completed, nor how the data reduction software pipeline and algorithms will utilize the data generated by SCal. Further analysis may reveal that additional calibration infrastructure is necessary to achieve the MSE science requirements. Prior to the preliminary design phase a "Calibration Feasibility" study considering the current MSE calibration plan, telescope and spectrograph designs, science requirements, and the calibration hardware proposed in this study in a holistic manner will be performed to ensure that the stated scientific goals of the MSE project are met. This report should be considered the next step in an iterative design process between the MSE science requirements, current optical and opto-mechanical concepts, and calibration and data reduction plans.

Further author information: (Send correspondence to L.M.S)

L.M.S.: E-mail: lmschmidt@tamu.edu, Telephone: 1 979 845 4401

2. SCAL FUNCTIONAL OVERVIEW & REQUIREMENTS

Figure 1 shows the SCal Work Breakdown structure. The majority of the work packages would be completed by the SCal design team, however both software and auxiliary calibration systems (in particular any detector illumination systems contained within the spectrographs) would be better led by the software and spectrograph teams and would include significant coordination with the SCal design team.

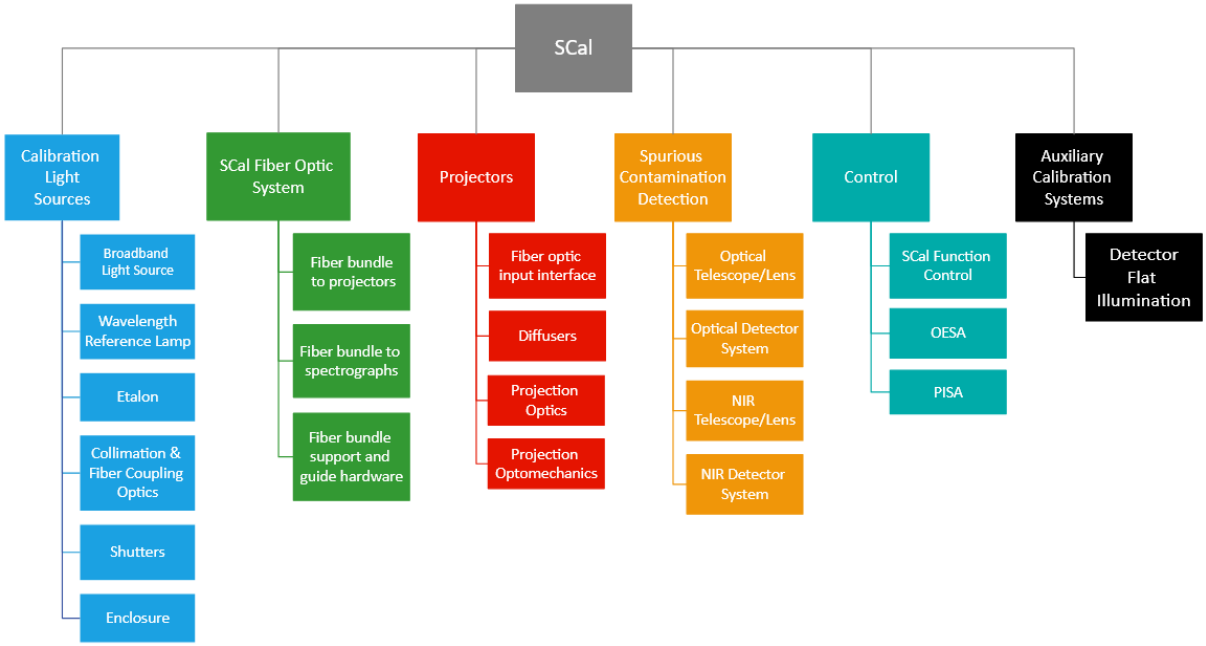

Figure 1. The SCal Work Breakdown Structure

SCal will interface with a variety of observatory systems, these interfaces may include these categories.

- Location
- Optical Interfaces
- Mechanical Interfaces
- Access and Handling Interfaces
- Communication, Software, and Control Interfaces
- Services and Utilities Interfaces
- Thermal Interfaces
- Operational Procedure and Process Interfaces

Currently identified interfaces between SCal and other subsystems are listed in the MSE SCal Design Requirements document (internal MSE document) and include key interface types identified above. In future design stages each interface will have an associated Interface Control Document.

Figure 2 is an overview of the connections between SCal and other MSE subsystems and the external environment.

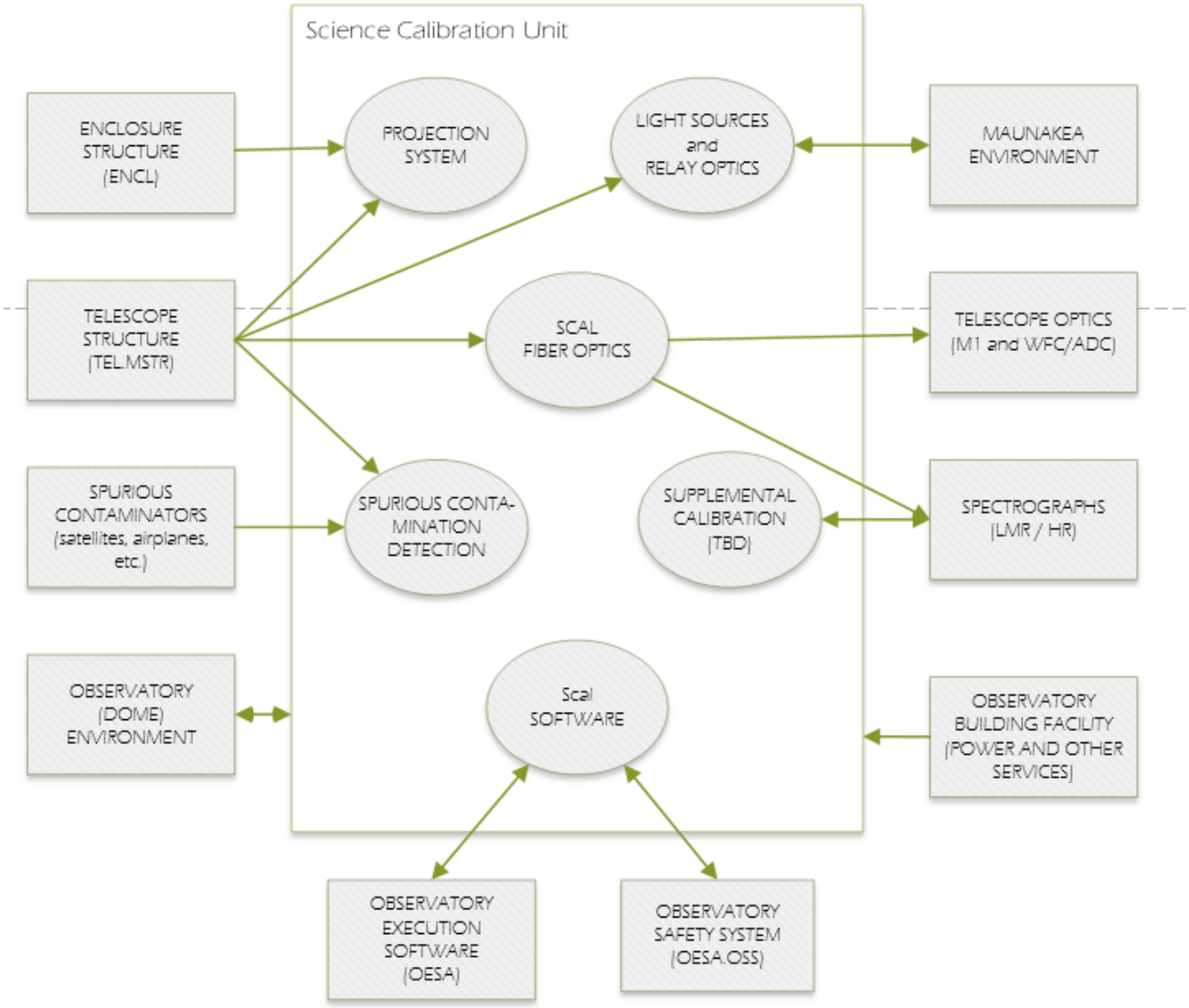

Figure 2. SCal Context Diagram, showing the major interfaces with other MSE subsystems.

3. SUBSYSTEM ARCHITECTURE

Each SCal subsystem is described below, including each of the considered solutions. Within each section the possible configurations are listed in order of increasing compliance/preference with the recommended configuration listed last. Summary tables are included to provide a high level comparison between the options that were evaluated.

3.1 FLAT FIELD LIGHT SOURCE

To achieve precise spectrophotometric calibration a broadband light source is required to calibrate system throughput. Any differences in transmission as a function of wavelength between fibers must be characterized. This light source has several key requirements.

- It must be sufficiently broadband to cover the full complement of MSE spectrometers from 360-1800 nm.

- It must be bright enough to ensure sufficient SNR is achieved during the calibration time allotment between science exposures.
- The output spectrum must be relatively flat to ensure all resolution elements are neither under nor over exposed during a calibration exposure.
- It must be long lasting, frequent light source changes due to failure or aging add maintenance overhead and down time and are a possible source of calibration errors.
- It must be stable; the output must be consistent to ensure calibration exposure times are predictable and do not require calibration time beyond the allotted calibration window between science exposures.

The following list of sources were considered. A brief description and reasoning for inclusion/exclusion from consideration are given for each source as well as commercially available examples.

3.1.1 Xenon

These lamps produce significant UV (UVA, UBV, UVC) light as well as ozone, both of which would require mitigation for safety reasons, depending on the location of the light source in the observatory. As MSE does not require calibration light at wavelengths shorter than 360 nm there is not a strong argument for choosing these lamps over other alternatives. Typical bulb lifetimes are on the order of 400-1000 hours. There is a warmup and stabilization time required that is significantly longer than the desired calibration time (minutes vs seconds). This means that the light source would stay on all night long, turning on and off with a shutter. With a mean bulb lifetime of 400-1000 hours, assuming a 10 hour/night average use, the bulbs would need to be replaced after 40-100 days. This replacement frequency adds additional maintenance requirements to the system.

3.1.2 Quartz Tungsten Halogen

These lamps do not produce as much UVA, UVB, and UVC light as Xenon lamps, or Ozone, but still cover the full wavelength range required by MSE. Stability is also better than Xenon lamps, however they still suffer from a limited lamp lifetime, on the order of 50-2000 hours. Typical filament sizes are on the order of mm's and could potentially work with a simple 1:1 reimaging optical system to inject light into the fiber array with many fibers leading to the projectors (a smaller source will require system magnification). However, when used with an etalon for wavelength calibration (discussed in section 3.2.4) the larger filament will result in a greater beam divergence when collimated and lower the resolution of an etalon. This could be overcome with spatial filtering, which would have the negative effect of loss of throughput.

3.1.3 LED

Broadband LED's offer a low power consumption, stable light source, with very long life, however there is not significant output above 1000 nm or below 400 nm in a single element (see Figure 3). Multi-LED sources are possible but would require combination of more than 10 separate LED's to achieve full coverage from 360-1800 nm. Generating a well collimated beam for an etalon would likewise be challenging due to the typical LED emitter size (typically a few mm's in size).

3.1.4 Supercontinuum Laser Light

Supercontinuum laser light is generated via propagation of short pulses through a nonlinear material, in most cases an optical fiber. One example is the Leukos Laser Samba UV supercontinuum laser, output spectrum is shown in Figure 4. Currently there is some concern with the overall spectral and temporal stability of supercontinuum sources,[4] but it is worth continued consideration as this technology is further developed. The expected lifetime of the laser is $>$ 20000 hrs at a very reasonable cost ($\sim$\$6000).

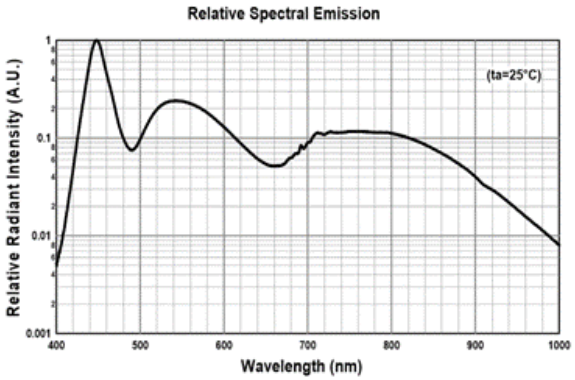

Figure 3. Ushio SMBBIR45A-1100-02 broadband LED output. The output drops significantly below 400 nm and above 1000 nm

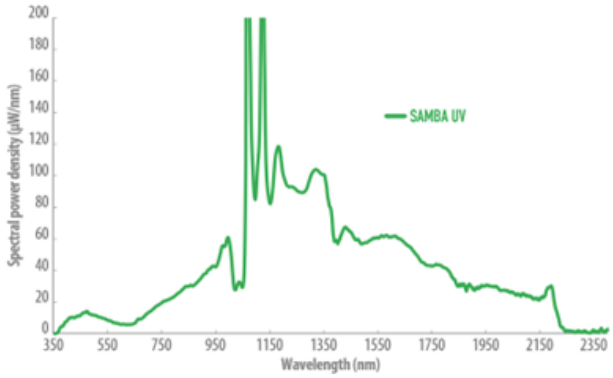

Figure 4. Leukos Laser Samba UV output spectrum. A custom filter may be required to reduce the intensity of the peaks around 1100 nm to ensure those wavelengths are not saturated during a typical calibration exposure time.

3.1.5 Laser Driven Light Source (LDLS)

The final source considered, and the recommended solution, is a laser driven light source (either Energetiq EQ-99X or ISTEQ XWS-65) in which an IR laser is used to heat a Xenon plasma source to higher temperatures, which results in a high output, broad spectrum source. Both options are available with a fiber optic output. There is some output loss with time (Figure 5), however most of the loss is in the UVB and UVC bands, which are not required for SCal and like a Xenon lamp must be filtered for safety. Energetiq recommends purging with dry Nitrogen (grade 4.8 or higher) as light below 200nm produces ozone in the presence of oxygen, and the ozone produced has an absorption band in the 220nm to 280nm range. To use light from the LDLS in the 170 to 280nm range, the system should be purged with high purity nitrogen. Purging with high purity nitrogen also reduces the possibility of photo-contamination of the bulb from trace organic vapors present in room air. MSE does not require this UV light, however Nitrogen purging may still be desirable for reducing the possibility of spectral contamination. For general safety, a longpass filter with cut on at 360 nm would be placed as soon as possible into the output beam to prevent exposure to UV light. Energetiq recommends changing the bulb after 10,000 hours of operation or once each calendar year, whichever comes first. The lifetime of the lamp / bulb is defined as when the intensity has dropped more than 50% at 500 nm. The spectral output at 500 nm decreases about 1% - 2% every 1,000 hours under standard operating conditions with nitrogen purging.

3.1.6 Source Flattening Filters

Recent advances in thin film coating allow for the creation of a custom “flattening” filter, which can transform the output of a light source into a very flat spectrum, removing any peaks in the spectrum through selective attenuation. The complete calibration system, including light source, relay and projection optics, fiber optics,

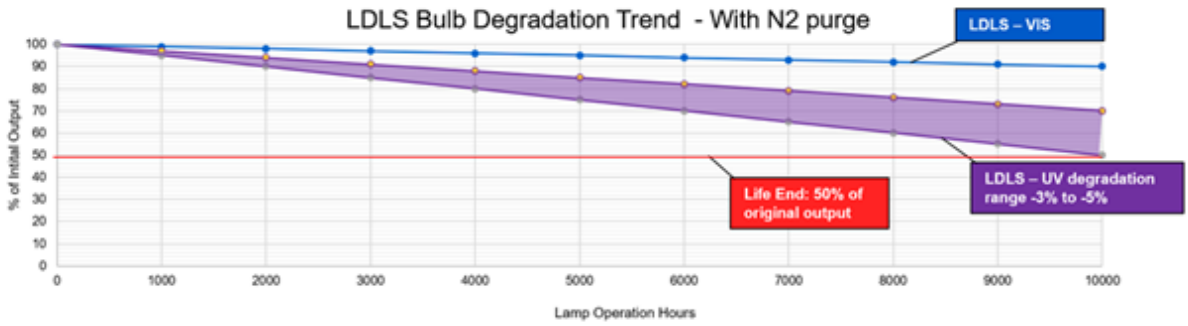

Figure 5. LDLS bulb degradation, image courtesy of energetiq.com/faq

etc. can be measured and the flattening filter designed to shape the final output spectrum and remove extreme output peaks. A theoretical filter design was produced by Alluxa Inc. to demonstrate what is possible, shown in Figure 6 and Figure 7.

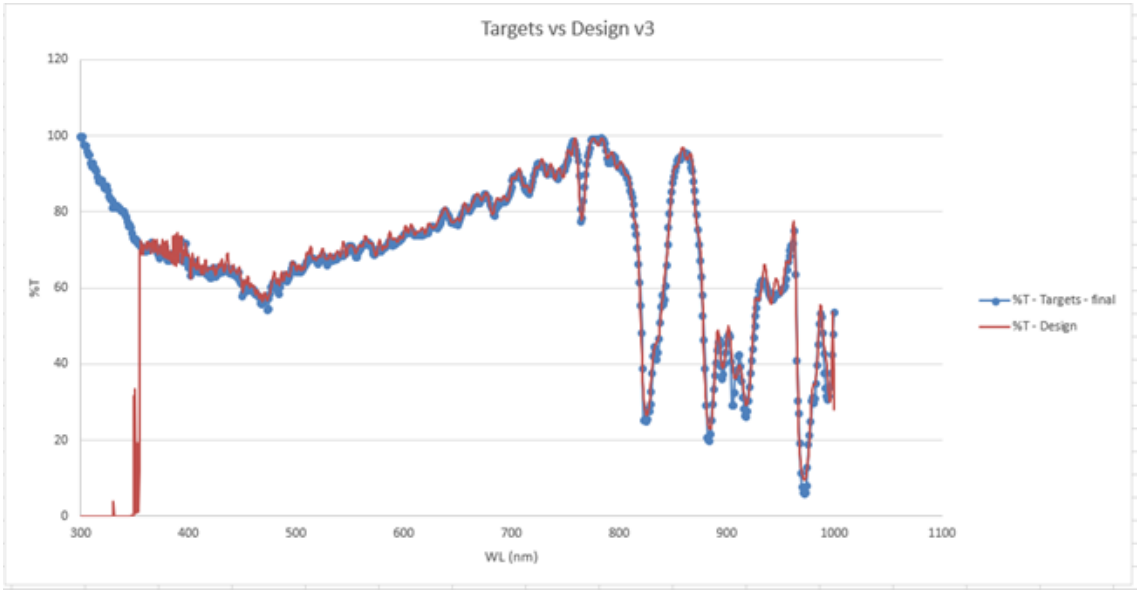

Figure 6. The target (blue) and design (red) transmission curves for a custom filter. In this case the design was limited to 350-1000 nm.

Because filters can only be subtractive, significant output is lost across the spectrum in the example that is shown, however this is weighed against the benefit of removing significant features in the original light source spectrum. The target filter response would likely be modified to consider losses within the calibration light transport optics and fiber optics. For example, fiber optic transmission drops significantly at blue/UV wavelengths, so the final filter curve would likely not cut wavelengths < 400 nm. Likewise, reducing the intensity of the peaks between 800 – 1000 nm in the LDLS while preserving the overall emission levels between 360-800 and 800-1800 nm will prevent those bands from saturating the detectors before the rest of the bands reach the desired SNR.

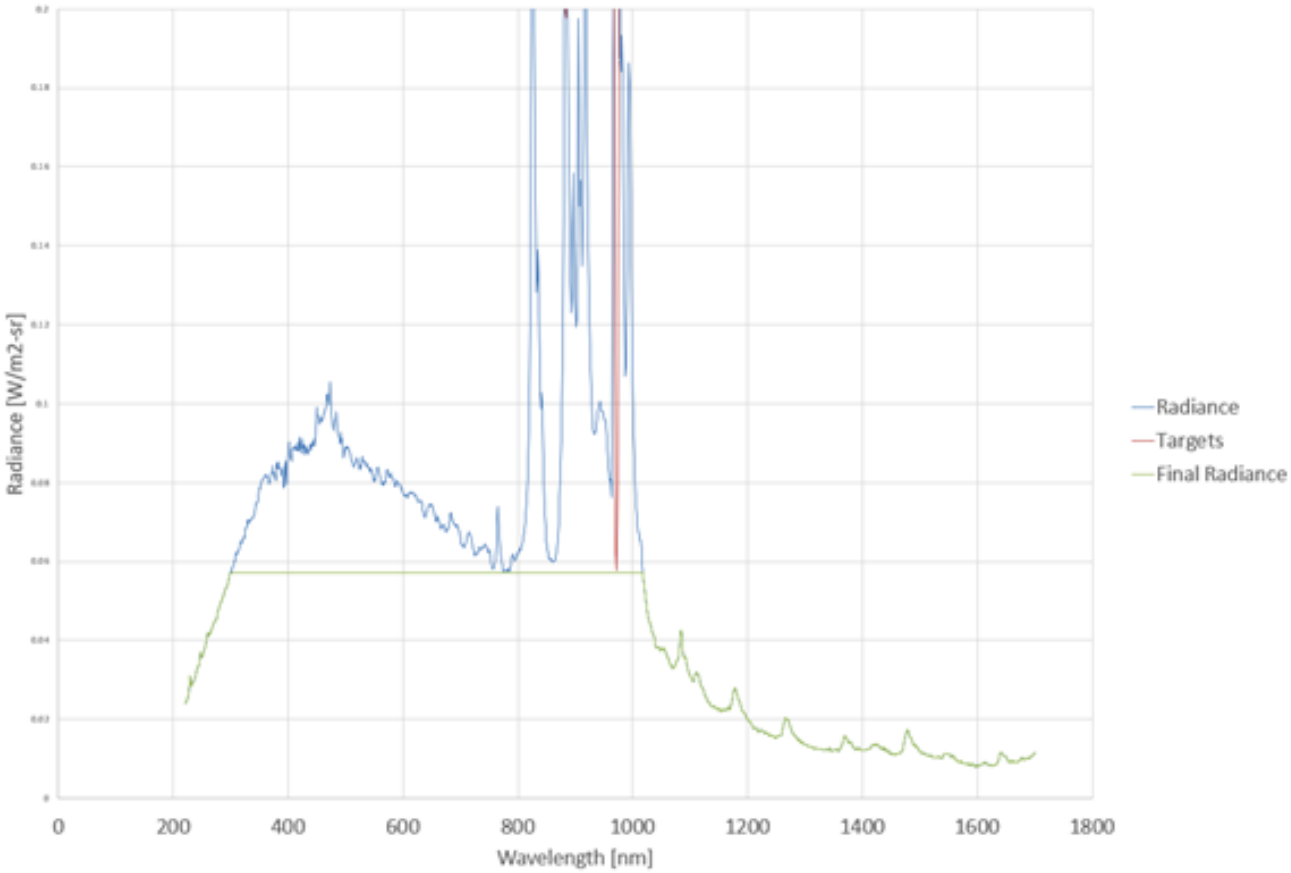

Figure 7. Both the original radiance and design targets are shown in blue and red. The final radiance is plotted in green. Notice the exceptionally flat resulting spectrum between 350 nm and 1000 nm. The SCal filter would likely be less extreme, only cutting the large peaks between 800 and 1000 nm.

3.1.7 Broadband Light Source Compliance Table

Table 1. Broadband calibration light source compliance table. Etalon is if the source is compatible with an etalon (the source size is small enough for low divergence when collimated).

Source	λ Coverage	Stability	Maintenance	Spectral Shape	Etalon
Xenon	✓	✓	×	✓	○
QTH	✓	✓	×	✓	○
LED	○	✓	✓	×	×
Supercont. Laser	✓	○	✓	✓ with flattening filter	✓
LDLS	✓	✓	✓	✓ with flattening filter	✓
Recommendation	✓ Compliant	○ Partially Compliant	× Not Compliant		

3.2 SPECTRAL CALIBRATION SOURCE

Generating scientifically useful data products will require precise wavelength calibration of each of the spectrographs. The ideal calibration source would have spectral lines that are evenly spaced, and of similar brightness across the full wavelength range of MSE.

3.2.1 Laser Frequency Comb

Laser frequency combs (LFC's) use mode locked lasers stabilized with a frequency standard to generate a "comb" of evenly spaced discrete spectral lines. They have the benefit of consistent line profiles and spacing, unlike the variability of traditional calibration lamps that can have blended lines and a wide range of line brightness. However, there are several significant drawbacks. The first is the cost, on the order of $1 million* for a complete system. The second is a limitation in wavelength coverage. Current LFC's do not work below 450 nm so for the blue channels of the various spectrographs (particularly the HR blue channel which covers 360-440 nm) an additional calibration source would be required for complete coverage. Finally, the typical frequency spacing of a LFC is on the order of 25-100 GHz or a line spacing of 0.03 – 0.12 nm, equivalent to 0.25-1 resel in the HR spectrograph. It may be possible to adjust the line spacing either through customization of the LFC itself, or pruning of the LFC with an etalon. This would be required in order to have reference lines spaced sufficiently for the wide range of MSE spectrograph resolutions ($R \sim 2500 - 40,000$). For these reasons LFC's are not recommended for MSE.

3.2.2 Lamps

Astronomers have used a variety of arc/hollow cathode lamps for spectrograph calibration; however they are not ideal sources for MSE as many have good calibration lines over only a limited spectral range (eg. Krypton 427-893nm, Neon 540-754nm), and may have many densely spaced lines leading to blended lines at low resolutions, or variable line densities so that portions of the spectrum do not have many calibration lines available. Most have multi-minute warm up times and short ($<$ 1000 hr) lifetimes before needing replaced. A combination of lamps could provide full wavelength coverage of the MSE spectrographs; however the constant lamp replacement is a maintenance burden (perhaps as often as monthly for some lamps). For these reasons arc/HCL lamps are not recommended as the sole wavelength calibration source for MSE.

3.2.3 Iodine Absorption Cells

Iodine absorption cells already have an established track record as a long term, stable reference. It would be relatively straightforward to insert an Iodine cell into the path of the broadband calibration light for projection into the telescope, or direct injection into the spectrographs. However, most of the spectral features are in the range of 500-620 nm and would not provide absolute calibration reference lines for all spectrographs.

3.2.4 Etalon and Reference Source

The recommended wavelength calibration source is the combination of a Fabry-Perot etalon inserted into the broadband calibration light in combination with a hollow-cathode lamp (HCL) to provide an absolute reference. The location of the etalon transmission peaks are dependent on the etalon temperature, tilt, etc. and can vary over time. Anchoring the etalon to an HCL allows for a long term stable solution. One combination is a Thorium-Argon HCL with etalon,[5] however recent changes in the manufacturing process of Th-Ar lamps has resulted in contamination by ThO molecular bands which results in portions of the spectrum being unusable for wavelength calibration. A better source may be Uranium-Argon or Uranium-Neon, which have line lists available covering 365-1700 nm,[6].[7] Another option that would not require replacement of an HCL lamp is locking the Fabry-Perot to a laser reference that is locked to an atomic transition.[8] The HCL does still have the replacement frequency concern, however it would be maintaining a single lamp, rather than multiple lamps, each with their own replacement lifetime. The FP would be located on a motion stage to allow it to be inserted into the collimated beam path of the broadband source. The HCL lamp would only be injected into the fibers going directly to the spectrographs to ensure sufficient signal is available for line fitting as the overall output of the HCL lamp is much less than the Energetiq light source. Using this method, it is possible to take wavelength calibration frames with the FP reference source in all spectrograph input fibers with relatively short exposure times ($< 10s$). A detailed trade in etalon performance will be required during preliminary design. In order to have an etalon that performs at all MSE wavelengths it is likely that metalized coatings will be required, and the desired finesse and free spectral range may be difficult to achieve over the broad range of wavelengths required. Additionally, the requirements of the LMR spectrographs and the HR spectrographs may require separate etalons

*Private Communication May, 2020 – Menlo Systems

to achieve the desired performance (for example a higher finesse is advantageous for the HR spectrographs to generate narrower peaks). This would require a more complicated "switchyard" to select the desired etalon and could impact the calibration efficiency if multiple exposures are required.

3.2.5 Wavelength Calibration Compliance Table

Table 2. Wavelength calibration light source compliance table.

Source	λ Coverage	Stability	Maintenance	Line Density
Laser Frequency Comb	×	✓	○	✓
Arc Lamps	✓	✓	○	○
Iodine Absorption	×	✓	✓	○
Continuum source & etalon	✓	✓ with temp. control	✓	✓
Recommendation	✓ Compliant	○ Partially Compliant	× Not Compliant	

3.3 CALIBRATION LIGHT OPTICAL RELAY

The broadband and wavelength calibration sources must be coupled to the telescope in some manner. It is most practical to locate the light sources somewhere near the telescope, or perhaps mounted to the telescope structure. The light sources then must be formatted for compatibility with the etalon (collimated), selection of broadband, etalon, or HCL source and coupled to fiber optics to transport the calibration light to the point where it is injected into the telescope. Figure 8 shows the conceptual layout of the calibration light sources and optics. Due to the extremely broadband calibration wavelengths, reflective optics (off-axis parabolas) are used for collimation and focusing. Likewise, optimizing the Fabry-Perot cavities for the broad wavelength coverage is challenging to optimize for all wavelengths due to the wavelength dependent nature ($\sim \lambda^2$) of the free spectral range (FSR) and the difficulty in producing optimized coatings for the broad range of wavelengths and spectrograph resolutions ($R \sim 2,500 - 40,000$). The right side of Figure 5 shows an option to split the broadband light, send it through two individually optimized Fabry-Perot's and recombine. The split wavelength requires optimization, however there is a gap in spectrometer coverage between 1320 nm and 1457 nm which is a natural transition point. The dual FP option would replace the single FP shown in the diagram on the left.

3.3.1 Coupling Optics

The light source coupling optics must accomplish several tasks including collimation of the light sources (fiber output of the LDLS and wavelength reference lamp) and focusing of the light onto the fiber bundles going to the projectors on the telescope, or directly injected into the spectrographs. Due to the broadband coverage of the calibration light, reflective off-axis parabolas (OAP) will be used to reduce coupling losses due to wavelength dependent focus shifts if lenses were used. Collimating the 0.22 NA output of the EQ-99XFC could be accomplished by a 25 mm diameter 50 mm focal length OAP which would result in a 22 mm diameter collimated beam. Injection into the fiber bundles going to the projectors or spectrographs would depend on the total number of fibers required. The focusing OAP focal length would be set by the magnification of the fiber output required to fully illuminate a hexagonal array of fibers. For example, using the 455-micron fiber output option, if the fiber bundle has a diameter of 2 mm, the required magnification is 2.0 / 0.455 = 4.4, so the required focusing OAP focal length is 4.4*50 = 220 mm. There are several beamsplitters required to pick off light to send to the spectrographs or introduce the HCL calibration light into the beam. Due to the broadband nature of the calibration light, coatings will be challenging, so a polka-dot Beamsplitter may be required, with a customized grid of reflective spots on the Beamsplitter to pick off the desired fraction of light. Alternatively if only a small fraction of the total output is required in the reflected beam, an uncoated window may be sufficient.

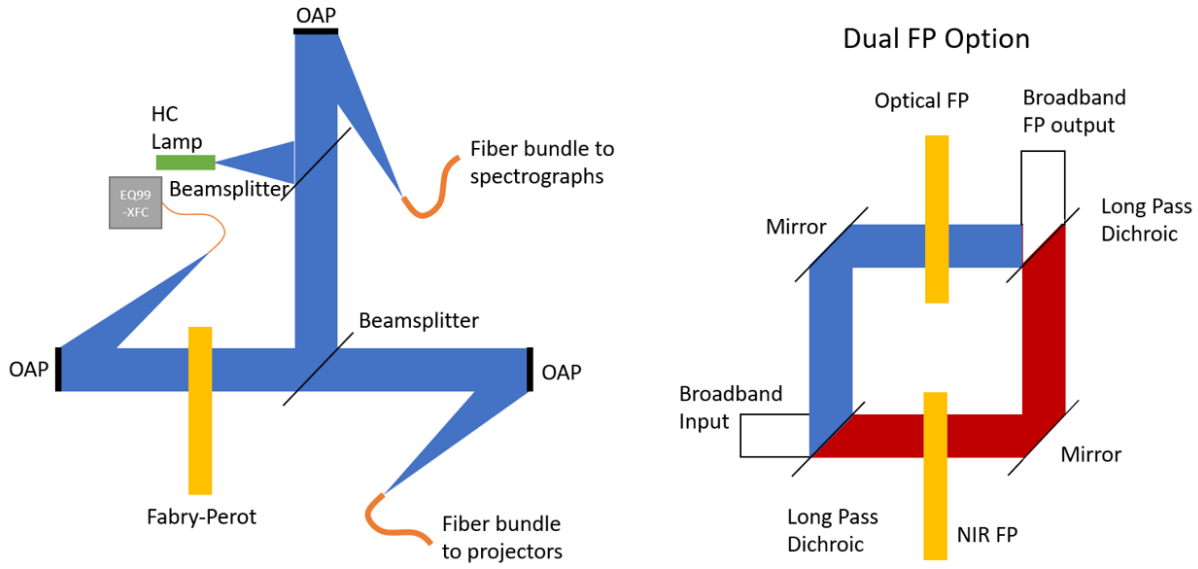

Figure 8. SCal layout on the left, on the right an option to replace the single Fabry-Perot with dual FP's, optimized for optical and NIR. Shutters would be placed before the output fiber bundles to selectively turn on/off the calibration light.

3.3.2 Fiber Optic Relay

The final decision on the fiber used in MSE has not been made, however it is likely a broad-spectrum fiber such as Polymicro FBP100120140 or similar will be used and this is adopted as the baseline choice in this study. Figure 9 shows the typical attenuation for this fiber, with very low losses over the majority of the MSE bandpasses. The peak at 1400 nm is not a concern as the cut-off of the NIR low resolution channel is 1320 nm and cut-on of the NIR moderate resolution spectrograph is 1457 nm. The highest expected losses will be in the 360-475 nm range. At 350 nm the loss is 70 dB/km which translates to 50% transmission at 43 m of fiber. There will be additional losses in the fiber from the positioner to spectrographs (50 m for HR and 35 m for LMR spectrographs). Considering these losses, minimizing the calibration light fiber lengths is important. If the calibration light sources can be co-located with the LMR spectrographs, 35 m of fiber length for the calibration light should be viewed as an upper limit. A system throughput estimation was calculated and uses the spectral power of the EQ-99XFC as provided by Energetiq as well as efficiency estimates for each optical component. The SNR is calculated for one resolution element at the central wavelength of each spectrograph channel. As expected, the lowest SNR is in each of the blue channels, due to the fiber optic throughput losses. However, SNR per resolution element is still between 950 and 2200 for 10 second exposures in the low and moderate resolution spectrographs and SNR of 280-900 for 20 second exposures in the high resolution spectrographs. The sensitivity of the high resolution blue spectrograph is the limiting case.

3.4 TELESCOPE LIGHT INJECTION SYSTEM

This system is responsible for taking the light from the calibration sources and after transporting it to the projection location via fiber optics, injecting it into the telescope.

3.4.1 Lambertian Screen

Due to the site constraints of the CFHT there is a relatively small gap between end of the telescope and inside surface of dome. This makes it very challenging to mount a traditional calibration screen to the inside surface of the dome and project even illumination over the full telescope aperture. A more important limitation of a dome mounted screen is the requirement for calibration exposures between science exposures. Requiring the rotation

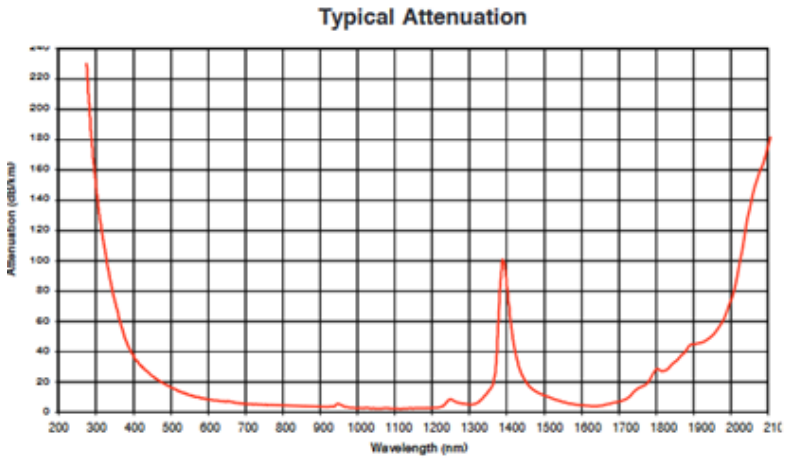

Figure 9. Typical Attenuation for Polymicro FBP100120140 broad spectrum fiber.

of the dome, or deployment of a moveable screen is not feasible in a reasonable time frame without severely impacting the overall survey efficiency. For this reason, a dome mounted screen was not seriously considered. There may be an argument for a dome mounted screen to be used for extended calibration activities during nights with weather related closures, however additional analysis is required to demonstrate the benefit of a dome screen flat field vs. sky flats.

3.4.2 M1 located point source

An array of point sources (for example a small integrating sphere and pinhole, or stand-alone fiber mounted facing the corrector) located in the spaces between mirror segments and co-located with the surface of M1 would remove the need for additional fiber bundles running to the top end of the telescope and could significantly reduce the required fiber lengths from light sources to telescope, however this location interferes with segment maintenance/removal and would require a much more distributed mounting of sources than mounting at the top end of the telescope. Top end mounting allows for a linear array along the fiber positioner support trusses, maintaining a compact fiber bundle. Distributed point sources at M1 would start as a bundle but must split (like the branches of a tree) and makes for a more complicated fiber routing problem. To avoid significant spillage of light past the corrector, illuminating the environment outside of the dome, baffling would be required and would result in significant throughput losses.

3.4.3 Integrating Sphere Linear Array

Located along the bottom side of each fiber positioner support at the top end of the telescope, a linear array of fiber fed integrating spheres and projection optics would provide collimated beams directed at M1 with the required beam divergence to illuminate the entire focal plane, with minimal spillage. The pupil is filled via azimuthal scrambling in the fibers going to the spectrographs. This system would be like that employed by the 4MOST project[9] which has already demonstrated a feasible design. Two drawbacks to this design are related to the extremely broadband nature of MSE and throughput concerns. The basic projector design is a small ($<$ 50 mm diameter) integrating sphere fed by a fiber optic. A small exit aperture ($\sim$1 mm) feeds an achromatic doublet which generates a collimated beam with the required divergence. The 4MOST project covers 370-950 nm so a commercially available doublet works well to collimate the light. MSE covers 360-1800 nm and it is difficult to find doublets that perform well at all of these wavelengths, many stock doublets use glasses with very low throughput at 360 nm ($<$ 20%) the Edmund Optics NUV-achromatic lenses are a notable exception. The most significant loss is due to the integrating sphere, which has $\sim$10% throughput. This requires $\sim$5x longer exposure times over several alternatives.

3.4.4 Engineered Diffusers

Engineered diffusers offer a potential solution to the low throughput of the integrating spheres while still offering most of the smooth illumination profile benefits of an integrating sphere. In the layout shown in Figure 10 a collimated beam lands on an engineered diffuser, placed at the front focal plane of a lens. The resulting illumination angle is set by the choice of engineered diffuser as well as the size of the incoming collimated beam. To aid in alignment simplicity and reduce cost relative to a second doublet lens, a fused silica ball lens is used to collimate the output from a fiber optic which then goes through an engineered diffuser placed at the front focal distance of an achromatic projection lens. Linear arrays of these projectors would be placed along the underside of each spider arm, offset from arm to arm, to fill the pupil more fully. A maximum of one hundred projectors on each arm (total 600) would be spaced 50 mm center to center. A few potential issues to consider are that there is some slight variation in the diffuser projection pattern with wavelength and if coherent sources are used, the diffusers produce speckle. Further modeling would be required to determine if a smaller number of projectors would still adequately fill the pupil.

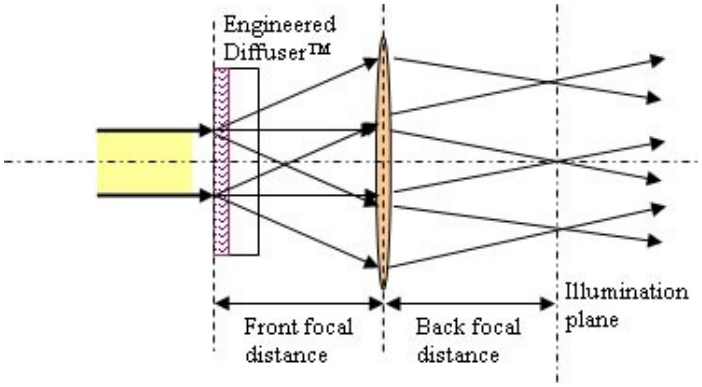

Figure 10. Telecentric illumination system layout, image courtesy of rpcphotonics.com. Fiber optic input and collimating ball lens would be to the left of this image.

3.4.5 Linear Fiber Diffusers

The end of a fiber optic may be converted to a linear diffuser via laser etching. This technology is available from several vendors, including Polymicro, a potential vendor for other MSE fiber optics. The end of the fiber has a laser engraved pattern which breaks the total internal reflection properties of the fiber and allows light to leak out of the sides of the fiber. Current processes limit the diffuser length to ∼50mm and typically each third of the diffuser outputs approximately the same amount of light. This process makes the end of the fiber fragile, so it is typically protected with a clear glass cylinder a few mm in diameter. Fiber diameter and type are customizable, so the same broad spectrum FBP fiber that is being considered for the spectrograph feeds may be used.

One drawback of using this as a source is that light is emitted in all directions from the etched surface of the fiber. To control this, the light could be constrained by a series of baffles or a mirrored coating on half of the protective glass cylinder that surrounds the fiber diffuser to direct light towards the primary mirror. Further exploration is necessary, but one possible configuration would be similar to “egg crate” grids used in overhead fluorescent lighting, or “bundle of straws” with the fiber diffusers placed at one end of the straws to control the light spread. This would require careful design to ensure spill outside of the M1 footprint is minimized but has the significant advantage that no other lenses, diffuser, etc. are necessary. It also allows for more complete radial pupil coverage and requires significantly fewer projection units when compared to the integrating sphere or engineered diffuser designs. Design of this type of projector is the most significant technological development required for this concept.

An example of the possible linear diffuser layout is shown in Figure 11. Opposite supports have a similar pattern, each pair covering 1/3 of the linear distance from the fiber positioner to the edge of the primary mirror. In practice, these baffles could be machined Aluminum, or perhaps even molded polycarbonate with a reflective

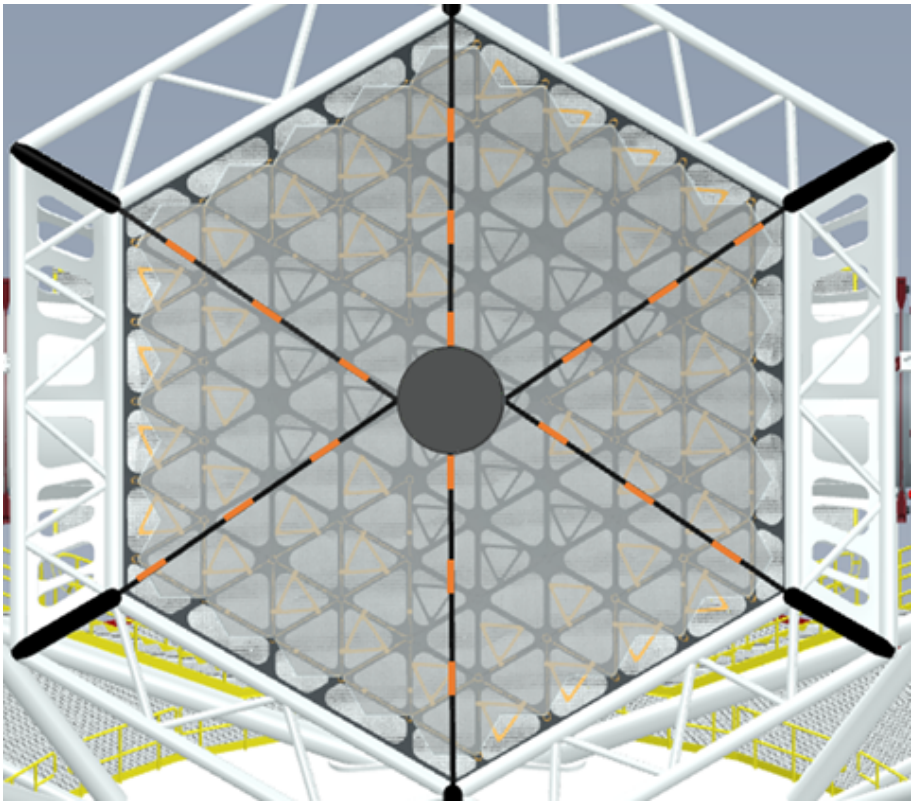

Figure 11. Layout of the fiber diffusers (orange), each segment would consist of multiple fiber diffusers mounted in a linear array. Each pair of supports fills $\sim 1/3$ of the radial profile and the pupil is filled via axial scrambling in the fibers.

coating (similar to a typical flashlight reflector). Prototyping and modeling will be necessary in the PDP. The fiber diffuser would be held at both ends of the diffuser portion by small standoffs (again, much like a fluorescent tube light fixture). In each of the top end mounted projection systems described above, the radial illumination profile must be adjusted to account for the difference in illuminated pupil area (projectors around the outside edge must be brighter or more densely packed than those located close to the center).

3.4.6 Projection Compliance Table

Table 3. Projection compliance table.

Injection Optics	Throughput	Mechanical Space	Achromaticity	Opening Angle
Lambertian Screen	○	×	✓	×
M1 point source	✓	○	✓	✓
Integrating sphere array	○	✓	✓	✓
Engineered Diffusers	✓	✓	○	✓
Linear Fiber Diffusers	✓	✓	✓	✓with baffle control
Recommendation	✓ Compliant	○ Partially Compliant	× Not Compliant	

3.5 TRANSIENT DETECTION SYSTEM

The large field of view and extremely faint detection sensitivities of MSE means that the likelihood of transient phenomena being captured during a science exposure and contributing enough signal to contaminate a science exposure is relatively high. A captured event may also not be easily detected through inspection of the spectra as the transient signal on a short timescale may have similar integrated flux as a faint target over the course of a typical science exposure. Because the telescope focal plane is sparsely sampled by the fibers and all the fibers go to spectrographs, it is not possible to easily inspect a science image for transient events, as is done with a typical imaging survey. Of particular concern is the proliferation of low earth orbit (LEO) satellite constellations, such as Starlink, OneWeb, Amazon Kuiper, and others that will populate LEO with thousands of satellites. These and other similar transients (airplanes, meteors) trace a path across the field of view, potentially impacting a relatively small subset of fibers. Other phenomena could impact all fibers, for example a lightning flash on the horizon, or a passing cloud.

To detect these events, the Transient Detection System (TDS) must be able to view the entire MSE field of view and must be constantly monitoring with a minimum of "dead" time. A long readout time for a detector is undesirable, a meteor crossing the field of view could be completely missed by a system with a readout time of several seconds.

An important consideration is also how the field of view is sampled. One might initially consider sampling at a fine enough resolution to match a TDS pixel to an individual fiber (∼1"/px sampling). This is certainly within reach using a $6k \times 6k$ pixel detector (1.52° FoV≈ 5500 px at 1"/px), however for moving point sources, such as a LEO satellite, the ultimate sensitivity is set primarily by the crossing time of the target on a pixel.

Figure 12 shows this peak in limiting magnitude vs exposure time in the case of a geostationary satellite and a sidereal tracking imaging system. This is a slightly different scenario in that the primary targets of concern are not geostationary, however, the argument still applies and the only difference is the pixel crossing time will be reduced for a non-geostationary target.

A satellite in a 550km (typical Starlink) orbit will take ∼ 24 seconds to cross the MSE field of view, which is ∼ 5 ms per arcsecond. To maximize the pixel crossing time, short focal length lenses are the best choice as the available pixel sizes are limited. In the trade-off between sampling and sensitivity, sensitivity is favored

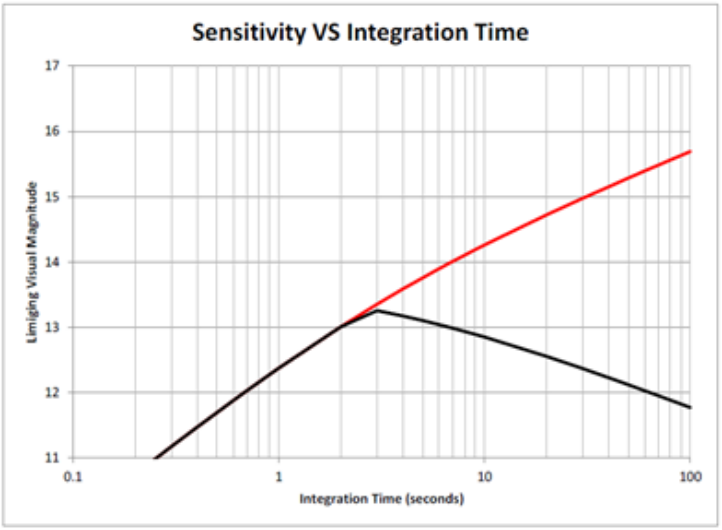

Figure 12. From Ackermann, Cox, McGraw, and Zimmer (2016),[10] calculations used a 135mm $f/2$ camera lens imaging a geostationary satellite while the camera system is tracking at the sidereal rate. The red curve is for a star, the black for the satellite. The decrease in limiting magnitude for the satellite at 3 seconds is due to the drift of the image across the detector. The pixel crossing time for the satellite image is 3 seconds.

over trying to achieve sampling that is equivalent to the expected fiber diameter (i.e. 1"/px). As long as the

sampling is fine enough to flag which fibers may be impacted, a more careful evaluation of the resulting spectra can determine if the satellite actually crossed the fiber, or perhaps the spectra is simply flagged to ignore, and the target is reobserved at a different time.

Table 4. Spurious contamination camera and lens combinations, SNR calculation assumes broadband/unfiltered images.

Optics/Camera	Px Crossing Time (s)	SNR 11.7 mag (AB)	Plate Scale (”/px)
Marana, Canon 200mm $f/2.8$	0.033	8.2	7.56
Marana, 8” RASA $f/2$	0.025	11.3	5.67
NIRVana, Stingray 200mm $f/1.6$	0.091	8.0	20.63

Table 4 lists several camera and optics combinations that could work to detect events. Two combinations for the optical (360-1000 nm) are given and one for the NIR (1000-1700 nm). The NIR camera does not cover the entire MSE wavelength coverage but extending past 1700 nm would require a much more expensive HgCdTe detector. The Andor Marana is a sCMOS camera with 2048 x 2048, 11-micron pixels, which are the largest available pixels in a CMOS sensor that comes packaged with thermoelectric cooling. CMOS is preferred over CCD due to the very short readout time ($\sim$ 20 ms). The Teledyne NIRVana InGaAs detector is thermoelectrically cooled with 640 x 512, 20-micron pixels. The Canon lens is chosen as a lens controller is available from Birger Engineering that allows for easy focus control. The Stingray SWIR lens would require a custom focusing solution (other lens models from Stingray include electronic focus control, so it is possible a packaged solution would be available). The Celestron RASA would also require a custom focusing solution.

Camera and lens combinations were evaluated using the PyETC package and included all known parameters of the detectors and lenses. Some values were estimated as no information was available (primarily optical throughput as a function of wavelength). For each combination, the SNR of a 11.7 magnitude (AB) target (based on estimates from Barden et al.[11]) with exposure time equal to the pixel crossing time was calculated.

Despite the longer pixel crossing time, the 300 mm lens has a lower SNR, simply due to the the additional sky background from the larger pixel and smaller aperture when compared to the Celestron RASA telescope. In the NIR this effect is even more noticeable due to the larger contribution of the sky due to the much larger pixels and image scale. The sky signal has a much larger impact as the source is very under sampled, so increasing the focal length reduces the sky background contribution without sacrificing any signal from a point source target. The allowed focal lengths in the NIR are limited due to the smaller number of pixels available in relatively low cost NIR detectors and the need to sample the full MSE field of view.

Each camera and optics combination are compact (fits within 250 x 250 x 750 mm) and can be mounted to the telescope structure in a variety of positions. One possible operational mode is each camera running in a circular buffer mode, where several sequential short exposures are averaged together and compared to new images as they are captured. Any difference between the images is flagged for further analysis, such as calculating which fibers may be impacted. The comparison image would need to be recaptured after every telescope position change. Both cameras are thermoelectrically cooled, so only require power and data connections.

The Celestron RASA telescope is not ideally suited for the Marana camera as the camera is large enough that it has additional vignetting (this telescope mounts the detector system at prime focus), but still has an overall advantage over the unvignetted Canon lens. As new camera models become available, it is possible a smaller camera would further improve performance by reducing the vignetting. If it is determined that only very short exposure modes will be utilized an uncooled camera for the optical bands may be sufficient and would offer significant size reduction. The RASA telescope consists of a spherical primary with a 4 lens corrector, optimized for the optical. It may be worth investigating the feasibility of a RASA telescope with custom corrector, optimized for the NIR, as an alternative to the Stingray lens.

3.6 LINESPREAD FUNCTION MAPPING

To remove the sky background from a target spectrum to better than 0.1% the variation in line spread function (LSF) across both wavelength and detector position must be characterized. The expected mode of operation requires ∼10% of the fibers, distributed across the field of view, to be dedicated to recording sky spectra. These sky spectra (or some average of several sky spectra) will be subtracted from the target spectra whose fibers are located nearby. However, the line spread function at a given wavelength will vary from fiber to fiber due to differences in FRD, focus, optical aberrations, etc., so the spectra must first be deconvolved from the line spread function for each fiber.

The change in LSF will likely be a smoothly varying function of field position and wavelength so it is not necessary to map the LSF at every field position and wavelength. Instead, sampling at discrete wavelengths for each fiber should allow for the LSF of unsampled wavelengths to be modeled.

3.6.1 Calibration Source for LSF Mapping

The ideal LSF mapping source is a regularly spaced set of spectral line sources, spectrally unresolved by the spectrograph that covers the full range of wavelengths in MSE.

3.6.2 Night Sky Lines

There are two options for calibration light when generating the line spread function maps. The first is using the night sky and calibrating using the sky lines as probes of the LSF. However, the night sky lines are not evenly spaced in wavelength and have a range of intensities which will result in variable LSF model precision, the line intensities also change with time. The other option is a facility generated light source, ideally one that is also used for other calibrations. For MSE, the wavelength calibration etalon source is the preferred solution. It has regularly spaced sources in wavelength, the projection system allows for all fibers to be mapped with the calibration source (including those directly injected into the spectrograph, which is not possible when using sky lines) and the absolute calibration source (lamp) can be turned off as the only mapping that matters is LSF at a given pixel location, knowledge of the exact wavelength at a particular pixel is not required. The following subsections describe several ways that the LSF can be determined using the etalon calibration source.

3.6.3 Grating Micro-stepping

It is possible to sample the LSF by micro-stepping the grating angle relative to the incoming beam when using a traditional reflection grating. Tilting the grating so that the LSF moves by 0.1 of a pixel as demonstrated on SINFONI[12] as well as on DEIMOS, NIRSPEC, and LRIS on Keck[13] super-samples the LSF and allows for reconstruction of the LSF. However, this method is not feasible with VPH gratings. As you tilt the grating, there is an efficiency change as a function of angle and wavelength (sometimes referred to as the “superblaze”) but tilting the grating without changing the camera collimator angle will not scan across wavelengths.

3.6.4 Detector Micro-stepping

This method produces essentially the same result as grating micro-stepping, however it is compatible with all grating types. The major downside to this method is the potential choice of catadioptric cameras for the MSE spectrographs where the detector is located inside the camera and the obstruction must be minimized. Adding the required mechanisms for micro-stepping in the available space will be a significant challenge but may ultimately be required to achieve detector alignment (tilt, focus, etc.). Detector micro-stepping in a completely transmissive camera is significantly easier as the vignetting by detector position mechanisms is no longer as much of a concern, however it still requires movement of a part of each spectrograph and for the highest level of precision focus, detector tilt, etc. must be maintained, only shifting the detector back and forth in the spectral direction, otherwise any measured LSF may be due to a change in focus, tilt, etc. from the nominal detector position used during science observations.

3.6.5 Tunable Laser

The current generation of tunable lasers offer broad (210 – 2300 nm) wavelength coverage and selection of any wavelength within that range with a narrow linewidth ($< 12\ cm^{-1} \sim 0.339$ nm at 532 nm). The tunable laser would need to be located in a temperature-controlled environment as the operating conditions required are 22°C ± 2 (Ekspla, model PT403). LSF calibration would involve injecting the laser light into the projection system and stepping through the calibration wavelengths. This has the advantage of being a single (tunable) wavelength at the possible expense of increased calibration time (though the brightness of the laser could enable calibration during the day). The etalon peaks are all produced simultaneously, where the tunable laser must step between wavelengths. This process is relatively fast, a 25 nm step in wavelength takes 250 ms[†] , or ∼15 s to step from 360 – 1800 nm in 25 nm steps. It is likely calibration time would be limited by the detector readout time, rather than the laser tuning time. A tunable laser would more than double the cost of the light source optical box, but would certainly be a flexible solution that could also be used for stray light characterization (see section 3.7.9).

3.6.6 Etalon Tuning

Etalon tuning is the preferred method for LSF calibration (for example, Kakkad et al.[14]) with the sky as a backup/complimentary source as that is available with the only cost being observing time. When considering the etalon for wavelength calibration, the uncertainty in etalon tilt, temperature, or spacing introduces uncertainty in the absolute wavelength calibration which is overcome with the addition of a hollow cathode lamp calibration source to anchor the wavelength calibration. To calibrate the LSF we take advantage of this inherent uncertainty to force small changes in the wavelengths of the etalon peaks to micro-step the etalon peaks across the detector allowing for super-sampling of the LSF as in Thatte et al.[12] and Kelson[13] unless the etalon has sufficient finesse that the peaks are unresolved by the spectrographs and no stepping is required. The change in wavelength of the peaks generated by the etalon is minimal when tuned and has the advantage that the spectrographs do not require any internal reconfiguration, only to take images as they would during any science observation. The etalon can be adjusted by varying the temperature, tilt, or thickness of the etalon (if air-spaced). Temperature is not desirable as the equilibration time will add significantly to the time required for a LSF characterization scan. The easiest method is fine adjustment of the etalon tilt relative to the incoming collimated beam. Extremely small angle changes can be introduced via a simple mechanical reduction and precision linear stage (short lever arm between pivot point and etalon, long lever arm between pivot point and actuator). These scans can then be deconvolved to extract the line spread function as a function of wavelength and detector position.

3.6.7 LSF Calibration Compliance Table

Table 5. Linespread Function calibration compliance table. Optical Configuration change: Does the calibration method require changes to the science light optical path (telescope-fiber-spectrograph system).

Source	Optical Config. Change	Calibration Time	Opto-mechanical Complexity
Grating Micro-Stepping	×	✓	○
Detector Micro-Stepping	×	✓	○
Tunable Laser	✓	○	✓
Etalon Tuning	✓	✓	✓
Recommendation	✓ Compliant	○ Partially Compliant	× Not Compliant

3.7 BACKGROUND CALIBRATION

3.7.1 Detector Characterization

Background calibration considers a variety of contributions to the recorded spectra. Several types of calibration are achievable without additional requirements placed on the spectrographs or calibration system beyond the

[†]Ekspla Lasers, private communication

inclusion of a shutter. These include detector dark current, pixel blemishes, and detector bias. These calibration frames can be captured using typical detector calibration techniques and will likely be quite stable. Initial calibration during commissioning will set the baseline values and can then be monitored on a regular basis for changes (quarterly, or perhaps even yearly in the case of bad pixel maps, bias frames require minimal capture time and may be collected at the beginning of every night).

One detector characterization task that may require additional hardware within the spectrographs is the characterization of the detector response. Any light entering the spectrographs, regardless of source, will only fall on a subset of pixels that map spatially and spectrally to the individual fibers along the slit. Without additional hardware it is impossible to illuminate the portions of the detector that fall between each of the spectral locations. Therefore, it is desirable to implement a method of completely illuminating the detector. It will also be necessary to decide if this detector illumination should illuminate all pixels with the same bandpass or simply spread out a broadband spectrum in the spatial direction to fill in the gaps between spectra. The preferred solution is best left to the spectrograph design and science calibration pipeline teams to decide as they have the most complete understanding of the space constraints within the spectrographs and calibration data needs.

There are two general types of illumination systems that were considered. The first is illumination using auxiliary LED's, the second is through additional fiber inputs into the spectrograph. The design of the LMR and HR spectrographs is still underway, and the ultimate design will determine compatibility with several of these concepts.

3.7.2 LMR Direct Illumination

One of the LMR spectrograph camera designs is shown in Figure 13. This catadioptric system places the detector inside of the middle optic. This means that the center of the left most optic is vignetted and an aperture could be cut to allow a light source to project directly onto the final corrector lens/detector. This source could be one or more LED's or an additional fiber from the calibration light source. Either source would diverge enough to illuminate the full detector, but a diffuser could be added inline to ensure even illumination. If the cameras are transmissive (as they are in alternative LMR designs, or the current HR design) this configuration will not work, as the LED's or fiber would vignette a portion of the beam.

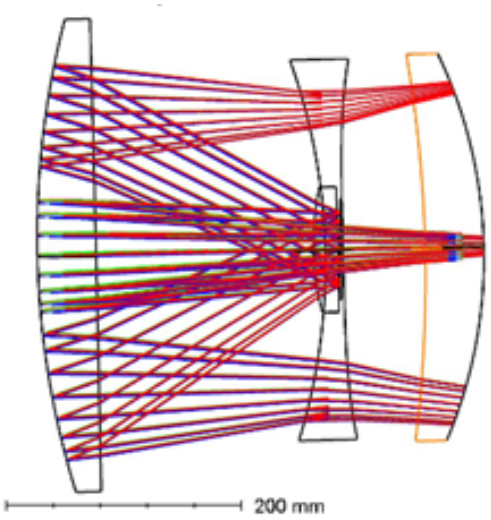

Figure 13. Detector Illumination: a source placed in a central aperture of the left most optic (Mangin mirror) would illuminate the entire detector.

An alternative that is compatible with either a transmissive or catadioptric optical design is modifying the shutter for each channel to include an illumination system. The back side (detector facing side) of the shutter

would be coated with a material such as Spectralon that has a Lambertian reflectance profile. When in the closed position, light would be projected from around the shutter aperture onto this surface, reflect off the back side of the shutter and into the camera. Depending on the location of the shutter, the illumination would likely be from very low angles relative to the shutter surface and would require multiple sources around the shutter aperture to achieve even illumination. Equivalent in some ways to a "ring light" commonly used in traditional photography. A potential downside is that if each channel has its own shutter, this system must be duplicated for each channel.

3.7.3 LMR Collimator Screen

A modification of the previous concept would allow for a single additional mechanism and provide detector flat calibration light to all channels simultaneously. Directly in front of the collimator mirror (see Figure 14) an additional shutter would be placed, once again with a reflective Lambertian surface on the side facing the cameras. When the shutter is closed, broadband calibration light is projected into the telescope, through the fibers and out of the fiber slit, illuminating the screen and reflecting off to pass through the dichroics, gratings, and cameras as usual, fully illuminating the detectors. This has the advantage of better on-axis illumination of the calibration screen as well as requiring only a slight modification of a standard part (coating one side of the shutter blade), but does require adding an additional shutter mechanism.

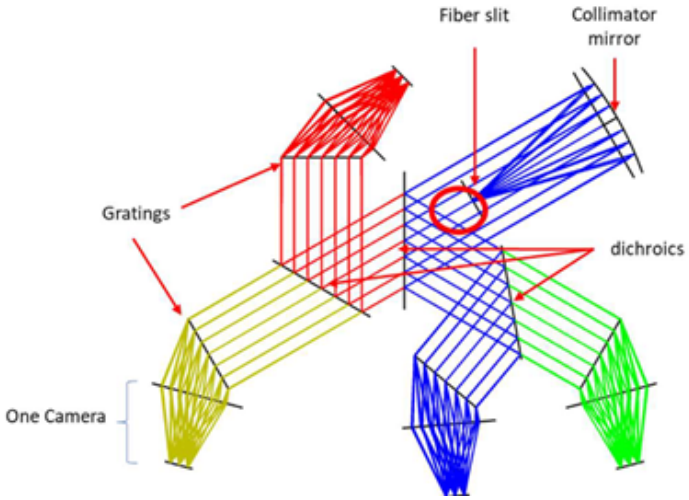

Figure 14. LMR Spectrograph layout from the conceptual design review held in 2021.

Alternatively, an internal LED source directed at a shutter screen in the same location would provide a diffuse illumination source to back illuminate the fiber slit.

3.7.4 Fiber Optic Slit Defocus

If a glass plate of sufficient thickness is inserted just after the fiber slit, defocus is introduced, blurring the spectra and illuminating a portion of the detector between spectral footprints. The amount of defocus will depend on the available space for the glass plate and insertion mechanism. Insertion of a plate is preferred over moving the fiber slit or detector to defocus as it does not require the spectrograph (fiber slit position, detector position, etc.) to be altered from the default configuration which could introduce systematic errors.

3.7.5 Transient Detector Calibration

Other background sources are variable in time and location on the detectors such as signals from radiation/cosmic ray events. Well established methods for removal exist and one step of the calibration pipeline must include identification and removal of these signals. A summary of several techniques for "impulsive noise removal" is included in Popowicz et al.[15] Currently additional calibration hardware does not appear to be necessary for transient detector calibration.

3.7.6 Ghosts and Scattered Light

To understand the contribution to the overall background signal from one or more fibers illuminated with a bright target (relative to a m=24, target in a particular field) or many faint targets, it would be advantageous to enable illumination of each fiber individually while blocking all the other fibers. This would allow a mapping of stray light from a particular fiber to locations on the detector. This is possible at two locations, either at the fiber positioner, or within the spectrograph at the fiber slit.

3.7.7 Fiber Slit Selective Illumination

A very flexible solution would be the introduction of a microshutter array (like that found in NIRSpec on JWST) just in front of the fiber slit within each spectrograph. With a microshutter per fiber, any combination of fibers could be blocked. However, this solution is likely not feasible due to cost and complexity, several of the spectrograph designs have the fiber slit embedded in the collimator, so any mechanism must be very compact to minimize vignetting and a shutter failure would remove that fiber from service and could only be fixed by a new (expensive) shutter.

An angled slit, sliding across the fiber slit would selectively mask all fibers but the one in the slit, however, to isolate an individual fiber, the slit must be close to the fiber slit and at a sufficient angle so that multiple fibers are not uncovered. This would not be compatible with a fiber slit embedded in the collimator optical path as the mechanism would vignette a significant portion of the collimated beam.

3.7.8 Fiber Positioner Selective Illumination

Space is also limited at the fiber positioner, but the required mask size is more easily manufactured. A moveable mask with a grid of apertures cut on the same pitch as the fiber positioners and placed just above the tips of the positioners would allow for selection of individual fibers by selectively tilting the fiber into the mask aperture directly above it, or to the side, under the mask as shown in Figure 15. The mask could be made from flexible

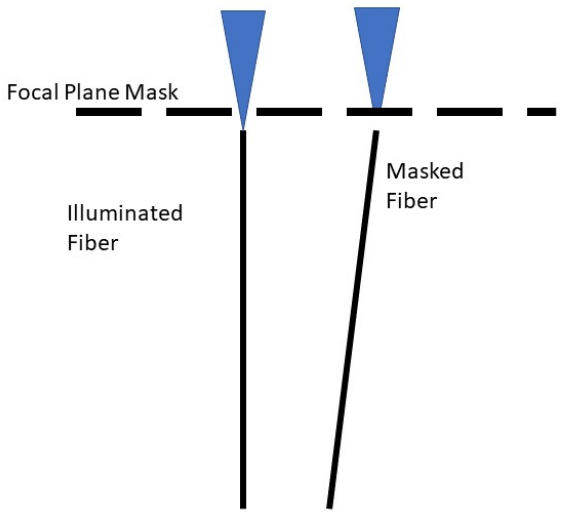

Figure 15. Sketch of a focal plane fiber mask for stray light characterization.

mylar and deployed like a roll out window shade, or as a solid Aluminum disk with machined apertures. An aluminum disk would require more space at the focal plane, or perhaps it could be deployed in multiple pieces, much like the blades of a camera shutter.

Perhaps the simplest (mechanically speaking) method would be to point the fiber being characterized at a bright star and point all the other fibers at blank sky. The main disadvantages of this method are the requirement to perform this calibration during the night (ideally during dark time to minimize the sky brightness) and the potential for confusion of stray light with sky background from the other fibers. Discussion with the positioner design team is required to determine the feasibility of a focal plane mask.

3.7.9 Monochromatic Stray Light Characterization

Finally, stray light as a function of wavelength can be characterized using monochromatic light sources at multiple wavelengths as described in Zong et al.[16] The calibration process starts by inputting monochromatic light into the spectrograph. Any signal that is recorded and not at the expected spectral line location is stray light. Scattered light is generally a smoothly varying function, so there is no need to step through every wavelength, the wavelength steps in Zong et al.[16] were every $\sim$ 8 nm (80 wavelengths between 200-800 nm). Sampling in this manner gives the advantage of more easily scaling the stray light model as a function of wavelength which can be matched to the scattering source spectrum. A trade study would be required to determine if multiple laser sources would be feasible, or if a tunable laser would be a simpler (though likely more expensive) approach. Investigation of this method during the calibration feasibility study would also be recommended, to determine if this method would provide a significant advantage to justify the additional hardware cost (>$100,000 for a tunable laser).

4. NEXT STEPS

The SCal conceptual design has identified a number of hardware solutions compatible with the MSE science goals and current calibration plan. After a "Calibration Feasibility" study is completed, which includes revising the current calibration plan, complete flow down of the MSE Science Requirements, and an updated data reduction pipeline plan, the SCal hardware design can be updated and the preliminary design phase can begin. We expect a significant modeling and prototyping effort for the projection system as well as finalization of the SCal requirements and interface documents during preliminary design, as well as updates to cost, schedule, and project risks.

ACKNOWLEDGMENTS

Texas A&M University thanks Charles R. '62 and Judith G. Munnerlyn, George P. '40 and Cynthia Woods Mitchell, and their families for support of astronomical instrumentation activities in the Department of Physics and Astronomy. The authors are grateful to Kei Szeto and Alexis Hill for helpful discussions and the conceptual design review team of Greg Barrick, John Pragt, Laurent Le Guillou, Arlette Pécontal, and Marc Baril for their feedback and discussion during the review process.

REFERENCES

[1] de Jong, R. S., Agertz, O., Berbel, A. A., Aird, J., Alexander, D. A., Amarsi, A., Anders, F., Andrae, R., Ansarinejad, B., Ansorge, W., Antilogus, P., Anwand-Heerwart, H., Arentsen, A., Arnadottir, A., Asplund, M., Auger, M., Azais, N., Baade, D., Baker, G., Baker, S., Balbinot, E., Baldry, I. K., Banerji, M., Barden, S., Barklem, P., Barthélémy-Mazot, E., Battistini, C., Bauer, S., Bell, C. P. M., Bellido-Tirado, O., Bellstedt, S., Belokurov, V., Bensby, T., Bergemann, M., Bestenlehner, J. M., Bielby, R., Bilicki, M., Blake, C., Bland-Hawthorn, J., Boeche, C., Boland, W., Boller, T., Bongard, S., Bongiorno, A., Bonifacio, P., Boudon, D., Brooks, D., Brown, M. J. I., Brown, R., Brüggen, M., Brynnel, J., Brzeski, J., Buchert, T., Buschkamp, P., Caffau, E., Caillier, P., Carrick, J., Casagrande, L., Case, S., Casey, A., Cesarini, I., Cescutti, G., Chapuis, D., Chiappini, C., Childress, M., Christlieb, N., Church, R., Cioni, M. R. L., Cluver, M., Colless, M., Collett, T., Comparat, J., Cooper, A., Couch, W., Courbin, F., Croom, S., Croton, D., Daguisé, E., Dalton, G., Davies, L. J. M., Davis, T., de Laverny, P., Deason, A., Dionies, F., Disseau, K., Doel, P., Döscher, D., Driver, S. P., Dwelly, T., Eckert, D., Edge, A., Edvardsson, B., Youssoufi, D. E., Elhaddad, A., Enke, H., Erfanianfar, G., Farrell, T., Fechner, T., Feiz, C., Feltzing, S., et al., "4most: Project overview and information for the first call for proposals," *The Messenger* **175**, 3–11 (2019).

[2] Sugai, H., Tamura, N., Karoji, H., Shimono, A., Takato, N., Kimura, M., Ohyama, Y., Ueda, A., Aghazarian, H., de Arruda, M. V., Barkhouser, R. H., Bennett, C. L., Bickerton, S., Bozier, A., Braun, D. F., Bui, K., Capocasale, C. M., Carr, M. A., Castilho, B., Chang, Y.-C., Chen, H.-Y., Chou, R. C. Y., Dawson, O. R., Dekany, R. G., Ek, E. M., Ellis, R. S., English, R. J., Ferrand, D., Ferreira, D., Fisher, C. D., Golebiowski, M., Gunn, J. E., Hart, M., Heckman, T. M., Ho, P. T. P., Hope, S., Hovland, L. E., Hsu, S.-F., Hu, Y.-S., Huang, P. J., Jaquet, M., Karr, J. E., Kempenaar, J. G., King, M. E., le Fèvre, O., Mignant, D. L., Ling, H.-H., Loomis, C., Lupton, R. H., Madec, F., Mao, P., Souza Marrara, L., Ménard, B., Morantz, C., Murayama, H., Murray, G. J., Cesar de Oliveira, A., Mendes de Oliveira, C., Souza de Oliveira, L., Orndorff, J. D., de Paiva Vilaça, R., Partos, E. J., Pascal, S., Pegot-Ogier, T., Reiley, D. J., Riddle, R., Santos, L., dos Santos, J. B., Schwochert, M. A., Seiffert, M. D., Smee, S. A., Smith, R. M., Steinkraus, R. E., Sodré, L., Spergel, D. N., Surace, C., Tresse, L., Vidal, C., Vives, S., Wang, S.-Y., Wen, C.-Y., Wu, A. C., Wyse, R., and Yan, C.-H., "Prime focus spectrograph for the subaru telescope: massively multiplexed optical and near-infrared fiber spectrograph," *Journal of Astronomical Telescopes, Instruments, and Systems* **1**, 035001 (2015).

[3] DESI Collaboration, Aghamousa, A., Aguilar, J., Ahlen, S., Alam, S., Allen, L. E., Allende Prieto, C., Annis, J., Bailey, S., Balland, C., Ballester, O., Baltay, C., Beaufore, L., Bebek, C., Beers, T. C., Bell, E. F., Bernal, J. L., Besuner, R., Beutler, F., Blake, C., Bleuler, H., Blomqvist, M., Blum, R., Bolton, A. S., Briceno, C., Brooks, D., Brownstein, J. R., Buckley-Geer, E., Burden, A., Burtin, E., Busca, N. G., Cahn, R. N., Cai, Y.-C., Cardiel-Sas, L., Carlberg, R. G., Carton, P.-H., Casas, R., Castander, F. J., Cervantes-Cota, J. L., Claybaugh, T. M., Close, M., Coker, C. T., Cole, S., Comparat, J., Cooper, A. P., Cousinou, M. C., Crocce, M., Cuby, J.-G., Cunningham, D. P., Davis, T. M., Dawson, K. S., de la Macorra, A., De Vicente, J., Delubac, T., Derwent, M., Dey, A., Dhungana, G., Ding, Z., Doel, P., Duan, Y. T., Ealet, A., Edelstein, J., Eftekharzadeh, S., Eisenstein, D. J., Elliott, A., Escoffier, S., Evatt, M., Fagrelius, P., Fan, X., Fanning, K., Farahi, A., Farihi, J., Favole, G., Feng, Y., Fernandez, E., Findlay, J. R., Finkbeiner, D. P., Fitzpatrick, M. J., Flaugher, B., Flender, S., Font-Ribera, A., Forero-Romero, J. E., Fosalba, P., Frenk, C. S., Fumagalli, M., Gaensicke, B. T., Gallo, G., Garcia-Bellido, J., Gaztanaga, E., Pietro Gentile Fusillo, N., Gerard, T., Gershkovich, I., Giannantonio, T., Gillet, D., Gonzalez-de-Rivera, G., Gonzalez-Perez, V., Gott, S., Graur, O., Gutierrez, G., Guy, J., Habib, S., Heetderks, H., Heetderks, I., Heitmann, K., Hellwing, W. A., Herrera, D. A., Ho, S., Holland, S., Honscheid, K., Huff, E., Hutchinson, T. A., Huterer, D., Hwang,

H. S., Illa Laguna, J. M., Ishikawa, Y., Jacobs, D., Jeffrey, N., Jelinsky, P., Jennings, E., Jiang, L., Jimenez, J., Johnson, J., Joyce, R., Jullo, E., Juneau, S., Kama, S., Karcher, A., Karkar, S., Kehoe, R., Kennamer, N., Kent, S., Kilbinger, M., Kim, A. G., Kirkby, D., Kisner, T., Kitanidis, E., Kneib, J.-P., Koposov, S., Kovacs, E., Koyama, K., Kremin, A., Kron, R., Kronig, L., Kueter-Young, A., Lacey, C. G., Lafever, R., Lahav, O., Lambert, A., Lampton, M., Landriau, M., Lang, D., Lauer, T. R., Le Goff, J.-M., Le Guillou, L., Le Van Suu, A., Lee, J. H., Lee, S.-J., Leitner, D., Lesser, M., Levi, M. E., L'Huillier, B., Li, B., Liang, M., Lin, H., Linder, E., Loebman, S. R., Lukić, Z., Ma, J., MacCrann, N., Magneville, C., Makarem, L., Manera, M., Manser, C. J., Marshall, R., Martini, P., Massey, R., Matheson, T., McCauley, J., McDonald, P., McGreer, I. D., Meisner, A., Metcalfe, N., Miller, T. N., Miquel, R., Moustakas, J., Myers, A., Naik, M., Newman, J. A., Nichol, R. C., Nicola, A., Nicolati da Costa, L., Nie, J., Niz, G., Norberg, P., Nord, B., Norman, D., Nugent, P., O'Brien, T., Oh, M., Olsen, K. A. G., Padilla, C., Padmanabhan, H., Padmanabhan, N., Palanque-Delabrouille, N., Palmese, A., Pappalardo, D., Pâris, I., Park, C., Patej, A., Peacock, J. A., Peiris, H. V., Peng, X., Percival, W. J., Perruchot, S., Pieri, M. M., Pogge, R., Pollack, J. E., Poppett, C., Prada, F., Prakash, A., Probst, R. G., Rabinowitz, D., Raichoor, A., Ree, C. H., Refregier, A., Regal, X., Reid, B., Reil, K., Rezaie, M., Rockosi, C. M., Roe, N., Ronayette, S., Roodman, A., Ross, A. J., Ross, N. P., Rossi, G., Rozo, E., Ruhlmann-Kleider, V., Rykoff, E. S., Sabiu, C., Samushia, L., Sanchez, E., Sanchez, J., Schlegel, D. J., Schneider, M., Schubnell, M., Secroun, A., Seljak, U., Seo, H.-J., Serrano, S., Shafieloo, A., Shan, H., Sharples, R., Sholl, M. J., Shourt, W. V., Silber, J. H., Silva, D. R., Sirk, M. M., Slosar, A., Smith, A., Smoot, G. F., Som, D., Song, Y.-S., Sprayberry, D., Staten, R., Stefanik, A., Tarle, G., Sien Tie, S., Tinker, J. L., Tojeiro, R., Valdes, F., Valenzuela, O., Valluri, M., Vargas-Magana, M., Verde, L., Walker, A. R., Wang, J., Wang, Y., Weaver, B. A., Weaverdyck, C., Wechsler, R. H., Weinberg, D. H., White, M., Yang, Q., Yeche, C., Zhang, T., Zhao, G.-B., Zheng, Y., Zhou, X., Zhou, Z., Zhu, Y., Zou, H., and Zu, Y., "The DESI Experiment Part I: Science,Targeting, and Survey Design," *arXiv e-prints* , arXiv:1611.00036 (Oct. 2016).

[4] Arun, S., Choudhury, V., Balaswamy, V., and Supradeepa, V. R., "Stability analysis of high power, octave spanning, continuous-wave supercontinuum sources based on cascaded raman scattering in standard telecom fibers," *OSA Continuum* **1**(4) (2018).

[5] Cersullo, F., Coffinet, A., Chazelas, B., Lovis, C., and Pepe, F., "New wavelength calibration for echelle spectrographs using fabry-pérot etalons," *Astronomy & Astrophysics* **624** (2019).

[6] Ross, A. J., Crozet, P., Adam, A. G., and Tokaryk, D. W., "A uranium atlas, from 365 to 505 nm," *Journal of Molecular Spectroscopy* **369** (2020).

[7] Sarmiento, L. F., Reiners, A., Huke, P., Bauer, F. F., Guenter, E. W., Seemann, U., and Wolter, U., "Comparing the emission spectra of u and th hollow cathode lamps and a new u line list," *Astronomy & Astrophysics* **618** (2018).

[8] McCracken, T., Jurgenson, C., Fischer, D., Stoll, R., Szymkowiak, A., Bradford, J., and Rutter, W., [*Single-lock: a stable Fabry-Perot based wavelength calibrator*], vol. 9147 of *SPIE Astronomical Telescopes + Instrumentation*, SPIE (2014).

[9] Roelfsema, R., Pragt, J., ter Horst, R., Agocs, T., Bellido, O., Brynnel, J., Calcines-Rosario, A., Frey, S., Helmi, A., Herrewijnen, J., Houtsma, T., de Jong, R., Lehmitz, M., Murray, G., Musters, G., Navarro, R., Saviauk, A., Schnurr, O., Sharples, R., and Winkler, R., "Calibration system for the 4MOST multi object fiber-fed spectrographs ," in [*Ground-based and Airborne Instrumentation for Astronomy VII*], Evans, C. J., Simard, L., and Takami, H., eds., **10702**, 2412 – 2428, International Society for Optics and Photonics, SPIE (2018).

[10] Ackermann, M. R., Cox, D. D., McGraw, J., and Zimmer, P., "Lens and camera arrays for sky surveys and space surveillance," report (2016).

[11] Barden, S. C., Depoy, D. L., Flagey, N., Hill, A., Marshall, J. L., Petric, A. O., Schmidt, L. M., and Szeto, K., "Science calibration for highly multiplexed fiber-fed optical spectroscopy: update from Maunakea Spectroscopic Explorer," in [*Observatory Operations: Strategies, Processes, and Systems VIII*], Adler, D. S., Seaman, R. L., and Benn, C. R., eds., **11449**, 486 – 503, International Society for Optics and Photonics, SPIE (2020).

[12] Thatte, N., Scott, N., Houghton, R., Nuernberger, D., Abuter, R., and Tecza, M., [*Improving the observing efficiency of SINFONI and KMOS at the VLT by factors of 2 to 4: sophisticated sky subtraction algorithms*], vol. 8448 of *SPIE Astronomical Telescopes + Instrumentation*, SPIE (2012).

[13] Kelson, D. D., "Optimal techniques in two dimensional spectroscopy: Background subtraction for the 21st century," *Publications of the Astronomical Society of the Pacific* **115**(808), 688–699 (2003).

[14] Kakkad, D., Tecza, M., Thatte, N., Piqueras López, J., and Kendell, H., [*HARMONI: Characterising the line-spread-function with a tunable Fabry-Pérot etalon*], vol. 11451 of *SPIE Astronomical Telescopes + Instrumentation*, SPIE (2020).

[15] Popowicz, A., Kurek, A. R., Blachowicz, T., Orlov, V., and Smolka, B., "On the efficiency of techniques for the reduction of impulsive noise in astronomical images," *Monthly Notices of the Royal Astronomical Society* **463**(2), 2172–2189 (2016).

[16] Zong, Y., Brown, S. W., Johnson, B. C., Lykke, K. R., and Ohno, Y., "Simple spectral stray light correction method for array spectroradiometers¿," *Applied Optics* **45**, 1111–1119 (2006).